ICSV14
Cairns • Australia
9-12 July, 2007

14th International Congress on Sound & Vibration

USING STATISTICAL METHODS TO PREDICT TURBULENCE INDUCED SOUND AND VIBRATION IN AEROSPACE AND AUTOMOTIVE APPLICATIONS

Patrik Ragnarsson[1], Christophe Schram[1] Michel Tournour[1], David Freed[2], Sivapalan Senthooran[2] and Fongloon Pan[2]

[1] LMS International, Interleuvenlaan 68, 3001 Leuven, Belgium
[2] Exa Corporation, 150 North Hill Drive, Suite 2, Brisbane, CA, USA
Patrik.ragnarsson@lms.be

Abstract
Wind induced sound and vibrations are areas where a lot of research efforts are spent today. Due to the random nature of turbulent flow fields, a deterministic approach to the problem will just describe one of many possible solutions. To reduce statistical uncertainty and achieve a robust solution of a problem a large number of calculations can be performed (i.e. Monte Carlo simulations). The focus of this paper is on a method to simplify the calculations involved in using such stochastic approaches. The experimental and numerical test case consists of a plate-backed cavity where the rectangular plate is excited by a reattaching turbulent boundary layer, and is supported by a visco-elastic seal. The approach is based on a Power Spectral Density (PSD) loading using a Corcos model. The statistical parameters are calculated by processing deterministic flow data. These data consist of time-series wall pressure fluctuations (WPF) obtained by CFD simulations. The WPF time series were computed using Exa's PowerFLOW CFD software, whereas the Vibro-acoustic responses were computed using LMS Virtual.Lab and Sysnoise.

The agreement between the random acoustic method using the Corcos model and a normal deterministic method is quite good. The over all levels are similar, and the results from the deterministic calculation show, as expected, more fluctuations than the random acoustic results. The random acoustic method is in a sense a superposition of a large number of deterministic load cases, hence the more smooth and averaged curve.

1. INTRODUCTION

Turbulent loading of structures is a big issue in many engineering applications. The turbulent flow on the wings of an airplane and the turbulence initiated by the A-pillar of a car are just two examples of areas where it is important to have a good understanding of the turbulent flow field and its effects on the structures and the radiated noise. This paper is focusing on ways to use simulated flow data for vibro-acoustic response calculations. Using normal deterministic calculation methods on this type of stochastic problem is very time consuming. To achieve a robust solution a large number of flow simulations are needed. One way of doing this is to perform a so called Monte Carlo simulation. The method studied in this paper is a random acoustic method. The idea is to use one single flow simulation and to use a statistical approach when solving the vibro-acoustical problem. In this paper the Corcos model is used to describe the flow field in a statistical manner [1]. The average PSD of the surface pressure, the streamwise and spanwise decay rates and the flow convection speed are the parameters used to express the flow field in terms of surface pressure fluctuations. From these parameters a set of orthogonal (i.e. uncorrelated) excitations are calculated using truncated singular value decomposition. For each of these orthogonal excitations the response is calculated in a deterministic manner. Finally the results from all the different orthogonal excitations are combined together into a complete, statistically robust solution for the plate vibration and the radiated sound pressure.

2. THEORY

2.1. The Corcos model

A plate is excited by a turbulent boundary layer because the turbulence generates a fluctuating pressure field on the plate. Assuming stationary statistics of the wall pressure field, the resulting vibration response of the plate can be written as [2]:

$$G_{uu}\left(y_i, y_j, \omega\right) = \iint H^*_{u,F}\left(\frac{y_i}{x_\mu}, \omega\right)\Phi_{pp}\left(x_\mu, x_\upsilon, \omega\right)H_{u,F}\left(\frac{y_j}{x_\upsilon}, \omega\right)dA_\mu dA_\upsilon \tag{1}$$

where G_{uu} is the response of the plate, $H_{u,F}$ are the frequency response functions relating displacement at y_i and y_j with the excitation at x_μ and x_υ and Φ_{pp} is the turbulent boundary layer cross power spectral density function of the pressure fluctuations between all the loaded points. The superscript * denotes the complex conjugate transpose.

The frequency response function $H_{u,F}$ of the plate can be calculated in many different ways. In this paper a finite element model is used.

If a temporally stationary process and spatial homogeneity of the flow field are assumed the cross spectral density function of the pressure loading Φ_{pp} can be separated into an averaged auto power spectrum of the pressure loading $\overline{\Phi}_{pp}$ and a coherence function Γ between the excitation points x_μ and x_υ. The cross power function can then be re-written as:

$$\Phi_{pp}\left(x_\mu, x_\upsilon, \omega\right) = \overline{\Phi}_{pp}(\omega)\Gamma(\zeta_1, \zeta_3, \omega), \tag{2}$$

where ζ_1 and ζ_3 are the streamwise and spanwise distance between the excitation points x_μ and x_υ. Corcos [1] hypothesized that the coherence function could be separated into two parts: a streamwise coherence function and a spanwise coherence function:

$$\Gamma(\zeta_1, \zeta_3, \omega) = A\left(\frac{\omega\zeta_1}{U_c}\right)B\left(\frac{\omega\zeta_3}{U_c}\right) \tag{3}$$

where the functions A and B could be simple analytical expressions depending only on the convection speed (U_c), the angular frequency (ω), the distance between the excitation points (ζ_1 and ζ_3), and decay constants (α_1 *and* α_3):

$$A\left(\frac{\omega\zeta_1}{U_c}\right) = e^{-\alpha_1\left|\frac{\omega\zeta_1}{U_c}\right|}e^{\frac{i\omega\zeta_1}{U_c}} \quad \text{and} \quad B\left(\frac{\omega\zeta_3}{U_c}\right) = e^{-\alpha_3\left|\frac{\omega\zeta_3}{U_c}\right|}. \tag{4) (5}$$

In this work the Corcos model is used by identifying the auto power spectrum and the coherence function from the CFD simulations. As can be seen in the equations above, the parameters needed to get the estimate of the coherence function are the convection speed and the spanwise and streamwise decay rates.

2.2 Singular value decomposition

Given the results from the Corcos model above, the cross power spectral density function of the surface pressure can be calculated. To calculate the resulting response of the system, this random pressure load case is decomposed into a set of orthogonal (i.e. uncorrelated) deterministic load cases. The way to obtain this decomposition of the cross power spectral density function (or matrix) is to use the truncated singular value decomposition method. The truncated singular value decomposition (SVD) is defined by [3].

$$\Phi_{pp} \approx U_m \sigma_m V_m^* \tag{6}$$

Where Φ_{pp} is the n *by* n cross power spectral density matrix, $\boldsymbol{U_m}$ and $\boldsymbol{V_m}$ are m *by* m orthogonal matrices, superscript * denotes the complex conjugate transpose and $\boldsymbol{\sigma_m}$ is an m *by* m diagonal matrix where the diagonal elements are the singular values. The truncation error satisfies:

$$\left\| \Phi_{pp} - U_m \sigma_m V_m^H \right\| = \sigma_{m+1} \tag{7}$$

where $\boldsymbol{\sigma_{m+1}}$ is the (m+1) largest singular value of Φ_{pp}. The singular values are automatically sorted by descending order, which allows easy and precise error estimation. This means that after choosing a truncation error limit for the calculation it is straightforward to decide on the number of load cases needed to achieve this limit.

Since the load cases are orthogonal, the results from solving all of these load cases can be recombined to the response of the system corresponding to the average response of a large number of deterministic calculations.

3. TEST SETUP

The test setup is shown in Figure 1 below. A tilted fence is located upstream of a plate supported by visco-elastic seals. A complex frequency independent stiffness has been used to model the seal. This stiffness was modelled as a transverse spring with the stiffness set to $2.2 \times (1 + 0.25i)$ MPa [4]. The plate dimensions are (466x375x3.38) mm and it is made of aluminium. The fence is 52.5 mm high, 490 mm wide, tilted 55 ^{o} and located 490 mm upstream of the plate.

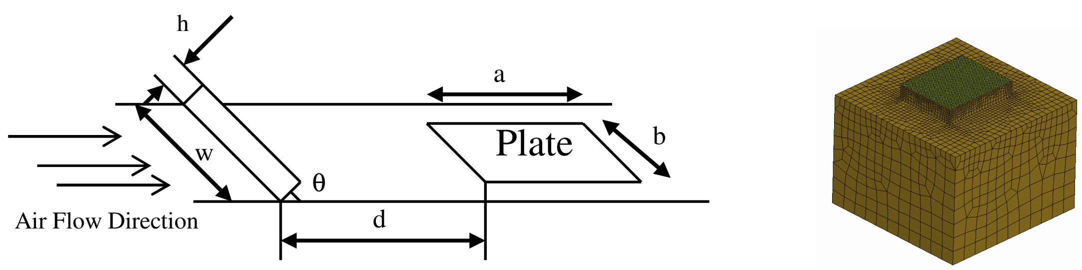

Figure 1. Left: The test setup, showing the plate downstream of the fence. Right: model of the cavity.

The plate mean-square velocity and the sound pressure level at a point 170 mm below the plate in a sound absorbing cavity were measured in the experiment.

4. CALCULATION PROCEDURE

4.1 CFD calculations

The exterior flow field and the pressure fluctuations on the plate surface were obtained from the simulation using the commercial software PowerFLOW 4.0a, from Exa Corporation.

4.1.1 Numerical Scheme

The underlying physics in PowerFLOW is based on the Lattice-Boltzmann Method (LBM) in which the fundamental equation of motion for fluid particles, the Boltzmann equation, is solved on a cubic lattice using a discrete set of fluid velocity states. The discrete Boltzmann equation is coupled with the ideal gas equation of state to represent realistic transfer of mass and momentum sufficient to describe small-scale fluid motions with very low numerical dissipation [5,6]. The geometry of the surface enters the LBM discretization as boundary facets immersed in the lattice, and they provide the boundary conditions for the discrete velocity states by enforcing zero-flux through the wall [7].

For high-Reynolds number turbulent flow, a turbulence model is used both for wall boundary layers and for dissipation of energy in the fluid to the scales of turbulence that can not be represented on the grid. The present approach can be thought of as "very large-eddy simulation" or VLES. The wall model uses a multi-layer boundary layer model with law-of-the-wall in the inner layer and the RNG k-epsilon model in the outer layer. The effect of surface pressure gradients is included through a local pressure gradient based rescaling of the usual law-of-the-wall; the resulting wall shear stress leads to correct prediction of boundary layer separation including when driven by a local adverse pressure gradient [8]. The VLES approach is achieved in the fluid domain by solving the RNG k-epsilon equations in the fluid, and coupling them to the Lattice-Boltzmann equations through the eddy-viscosity [9,10]. This VLES approach is capable of producing high-fidelity WPF up to very high frequency, where the desired frequency is limited mostly by the choice of grid resolution for the computational lattice. See, for example, Vaillant and Maillard [11], Senthooran *et al.*[12], and Belanger *et al.* [13] for further details.

4.1.2 Computational Methodology

The test configuration shown in Figure 1 was replicated in the PowerFLOW digital wind tunnel as shown in Figure 2. The simulation was done at 43.6m/s inlet velocity matching the experimental wind tunnel speed. Variable resolution regions were used with fine resolution in critical regions to predict the boundary layer development and flow separation accurately and coarse resolution in non-critical regions to optimize the computational effort. The finest cell size used in the simulation is 0.75 mm. The time step in this numerical scheme is inherently determined based on the resolution and Mach number. The simulation ran for 368,868 time steps, corresponding to 1 second in physical time. The transient surface pressure data on the plate was collected in such a way as to emulate 1.37 mm diameter microphones at the locations used in the experiment to validate the CFD calculations. These microphone locations are shown in Figure 2. The transient pressure data was recorded on the entire plate surface on a mesh with the grid size 5 mm for flow visualizations and to provide the data required for the vibro-acoustic calculation. These measurements were sampled at 36890 Hz and were recorded for 0.7 seconds.

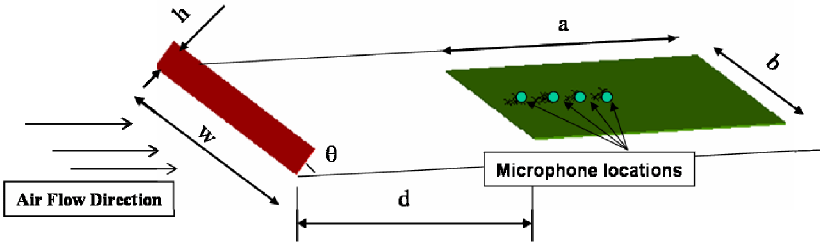

Figure 2: CFD configuration with microphone locations

4.2 Acoustic response calculations

The calculations have been performed in LMS Virtual.Lab and Sysnoise. The first step was to calculate the modal response of the structure in LMS Virtual.Lab. Thereafter the plate was loaded with a pressure field and the radiated sound could be calculated. The pressure loading were performed in two different ways: a deterministic approach and a random approach.

4.2.1 Deterministic approach

The procedure was to import the wall pressure from the CFD calculation and to transform it in to point forces distributed over the plate. These point forces represents the turbulent pressure fluctuation that drives the plate. Since the CFD calculations normally are performed with a very dense mesh, the acoustical mesh can be coarsened to save calculation time and memory use. The CFD data are then interpolated to fit the coarsened acoustical mesh. The interpolation procedure starts from a node on the coarser mesh; the eight closest nodes within a user defined maximum distance on the corresponding denser mesh are taken under consideration. These eight nodes are weighted based on the inverse of the distance from the new node according to (8)

$$x_{Ac} = \frac{x_1(1/d_1)+x_2(1/d_2)+x_3(1/d_3)+\ldots+x_8(1/d_8)}{(1/d_1)+(1/d_2)+(1/d_3)\ldots(1/d_8)}. \qquad (8)$$

Based on the new acoustical mesh with the corresponding point forces, the sound radiation problem could then be calculated by solving the coupled structure-acoustic model in LMS Virtual.Lab. The structure is solved with FE techniques and the acoustic problem is solved using BEM technique.

4.2.2 Random approach

The pressure field was represented by a cross power spectral density matrix which is derived from the well known Corcos model [1]. The Corcos parameters have been extracted from the CFD simulations (see Figure 6). The cross PSD matrix were then decomposed into a number of orthogonal load cases which combined represents the desired pressure loading. Each of these load cases can then be solved in a deterministic manner in a similar was as for the deterministic approach described above. The complete solution is obtained when the result from all the load cases are recombined to a final result. In LMS Virtual.Lab and Sysnoise the process of decomposing the data in to load cases, solving the load cases and recombining them is automatically performed in the random acoustic module.

5. RESULTS AND DISCUSSION

Figure 3 shows the time averaged velocity magnitude and streamlines on a plane on the centreline of the plate. This shows that the time-average flow reattachment is just past the leading edge of the plate, upstream to the microphone locations.

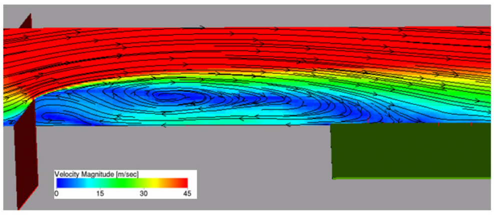

Figure 3. Time averaged velocity magnitude and 3D streamlines

Figure 4 shows the comparisons between the experimental and predicted power spectra density (PSD) for all four microphones located on the plate. For both the predictions and the measurements, the spectra are seen to depend only weakly on the streamwise location, indicating a fairly homogeneous turbulent field over that region. This implies that the assumption in Equation 2 about spatial homogeneity is at least valid over that region of the flow field. Both the experimental and simulations results show high pressure fluctuation levels below 100 Hz and continuous reduction in pressure fluctuation levels from 100 Hz to the high frequency region. The cascading slope predicted in the simulation agrees well with the experiment up to a very high frequency region. The amplitude of the simulation spectra are slightly over-predicted compared to the experimental spectra. This could be due to slight mismatch in the reattachment location between simulation and experiment. Another source of error could be a mismatch of the upstream boundary layer and turbulence levels; these were not characterized for experiment so they could not be matched in simulation;

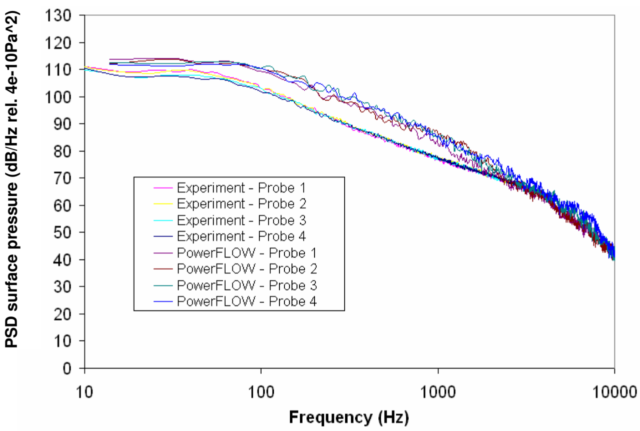

Figure 4: Power Spectra Density (PSD) of the plate surface pressure. Comparisons between PowerFLOW and experiment.

Pressure fluctuations on the surface of the plate due impingement of the transient flow structures can be characterized by dB-maps of pressure fluctuations on the surface. Figure 5 shows the dB-maps for the plate surface in octave bands. It can be seen that the complex pressure fluctuation topology on the plate surface is well captured and represented by these dB-maps compared to the microphone measurements taken at experimental locations.

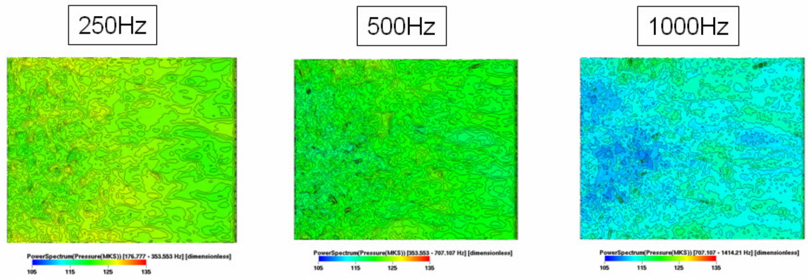

Figure 5: Octave band dB maps of the plate surface pressure

These pressure fluctuations predicted from the PowerFLOW simulation on the entire plate using a fine mesh were transferred to LMS Virtual.Lab in time domain for acoustic response calculations for the deterministic method and have been used to estimate the Corcos parameters for the random acoustic method.

The PSD of the average surface pressure can be seen in Figure 6 left. Figure 6 right shows the estimation of the convection speed of the turbulent flow field. The decay rates are estimated by fitting Equations (4) and (5) to the coherence function in spanwise and streamwise direction respectively. The decay rates were estimated to 0.3 in the stream wise direction and 0.7 in the span wise direction. This corresponds well to the decay rates from the measurements [4].

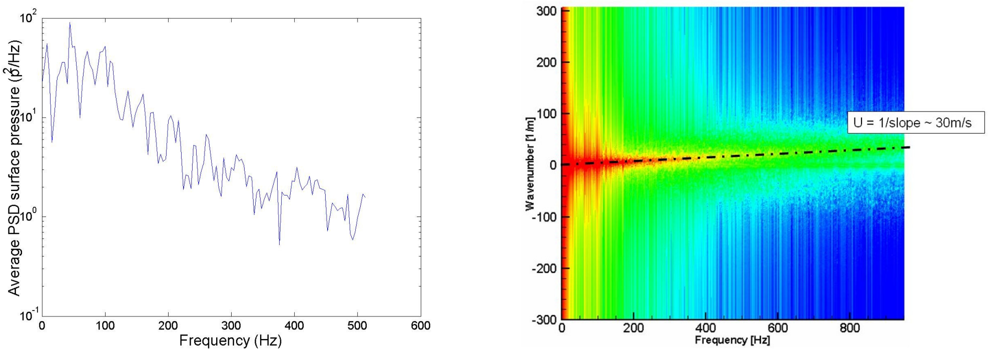

Figure 6: Left: PSD of the average surface pressure. Right: estimation of the convection speed of the turbulent flow field.

In Figure 7 left a comparison of the plate surface velocity can be found. Experimental results (blue) are compared with two simulation results; a deterministic approach (pink) and a Corcos approach (black). In Figure 7 right, the results from the sound pressure inside the cavity are presented. The calculations have been performed in the frequency range 75-500 Hz.

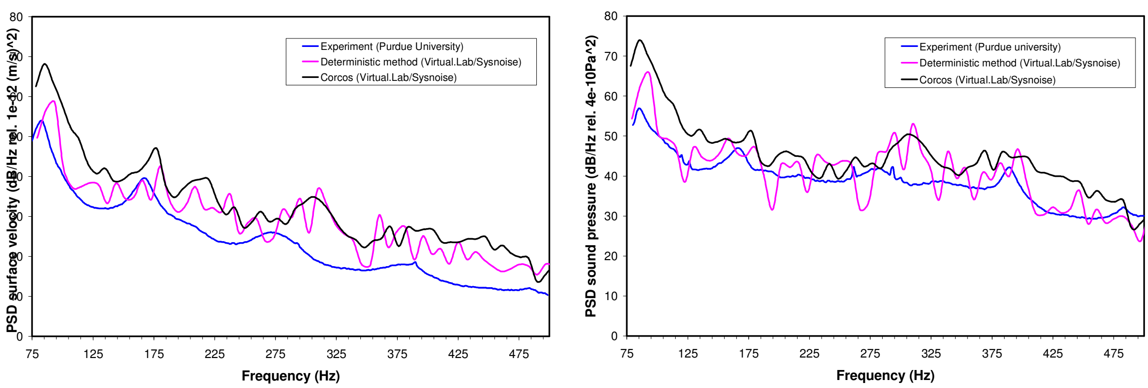

Figure 7: Comparison of calculation with a standard deterministic approach, The Corcos approach and experiments. <u>Left</u>: plate surface velocity <u>Right</u>: Sound pressure level in the cavity 170 mm from the plate

As it can be seen in Figure 7 both the deterministic calculation and the random acoustic calculation over predicts the results from the measurements. One possible reasons for this is the over prediction of the surface pressure in the CFD calculations.

In Figure 4 the calculated plate surface pressure at four microphone positions are compared with the measurements at these points. The CFD results are 5-10 dB-units higher than the measurements for the entire frequency range of interest. Keeping this in mind while looking at the plate velocity and the sound pressure in the cavity, the results match better.

6. CONCLUSIONS

The agreement between the deterministic method and the random acoustic method is quite good. As expected, the deterministic method shows more fluctuations than the random acoustic method. The random acoustic method is in a sense a superposition of a large number of deterministic load cases, hence the more smooth and averaged curve. The smoothness of the experimental curve is probably due to a large number of averages. Future experiments and calculations will be performed in order to address discrepancy between the experimental results and the simulations.

ACKNOWLEDGEMENTS

The authors gratefully acknowledge the EC support for the present work, performed within the Marie Curie EST project 'SIMVIA2' (www.simvia2.eu, contract nr MEST-CT-2005-020263).

REFERENCES

[1] G.M. Corcos, “The structure of the turbulent pressure field in boundary-layer flows”, Fluid Mechanics 18, 353-378 (1963).

[2] S.A. Hambric, Y.F. Hwang, W.K. Bonness, “Vibrations of plates with clamped and free edges excited by low speed turbulent boundary layer flow” *Journal of Fluids and Structures 19*, 93-100, 2003.

[3] Bendat J S & Piersol A C,“Random data: analysis and measurement procedures” New York: Wiley, 1971.

[4] J. Park, L. Mongeau, T. Siegmund, "An Investigation of the Flow-induced Sound and Vibration of Viscoelastically Supported Rectangular Plates: Experiments and Model Verification", Journal of Sound and Vibration 2004, 275, 249-265

[5] Y. Li, R. Shock, R. Zhang, and H. Chen, “Numerical Study of Flow Past an Impulsively Started Cylinder by Lattice Boltzmann Method”, J. Fluid Mech., Vol. 519, 2004, pp. 273-300.

[6] H. Chen, O. Filippova, J. Hoch, K. Molvig, R. Shock, C. Teixera, and R. Zhang, “Grid Refinement in Lattice Boltzmann Methods Based on Volumetric Formulation”, Physica A 362, pp. 157-167, 2006.

[7] H. Chen, C. Teixeira, and K. Molvig, “Realization of Fluid Boundary Conditions via Discrete Boltzmann Dynamics,” Intl. J. Mod. Phys. C, 9 (8), 1998, p. 1281.

[8] C. Teixeira, “Incorporating Turbulence Models into the Lattice-Boltzmann Method,” Intl. J. Mod. Phys. C, Vol. 9 No. 8, 1998, pp. 1159-1175.

[9] H. Chen, S. Kandasamy, S. Orszag, R. Shock, S. Succi, and V. Yakhot, “Extended Boltzmann Kinetic Equation for Turbulent Flows”, Science, Vol. 301, pp. 633-636, 2003.

[10] H. Chen, S. Orszag, I. Staroselsky, and S. Succi, “Expanded Analogy Between Boltzmann Kinetic Theory of Fluid and Turbulence”, J. Fluid Mech., Vol. 519, 2004, pp. 307-314.

[11] O. Vaillant, and V. Maillard, “Numerical Simulation of Wall Pressure Fluctuation on a Simplified Vehicle Shape”, AIAA Paper 2003-3271, 2003.

[12] S. Senthooran, B. Crouse, G. Balasubramanian, D. Freed, and S. Noelting, “Simulation Of Wall Pressure Fluctuations On Simplified Automobile Shapes Using A Lattice Based Method”, Proc. 2005 ASME IMECE, Nov. 5-11, 2005, Orlando, Florida.

[13] A. Belanger, M. Meskine, B. Caruelle, and K. Debatin, ”Aero-acoustic Simulation of a Double Diaphragm Using Lattice Boltzmann Method”, AIAA Paper 2005-2917, 2005.